Density functional approach to phonon dispersion relations and elastic constants of high-temperature crystals

1991 J. Phys.: Condens. Matter 3 9943

(http://iopscience.iop.org/0953-8984/3/50/001)

J. Phys.: Condens. Matter 3 (1991) 9943–9963. Printed in the UK

Density functional approach to phonon dispersion relations and elastic constants of high-temperature crystals

M Ferconi and M P Tosi
Department of Theoretical Physics of the University of Trieste and International Centre for Theoretical Physics, Strada Costiera 11, I-34014 Trieste, Italy

Received 29 July 1991

Abstract. The renormalized phonon frequencies of a monatomic classical crystal at melting are related to the direct correlation functions of its liquid at freezing by means of a functional expansion of the free energy of a suitably deformed crystal around the liquid phase. Expressions for the elastic constants follow by the 'long-waves' method and are compared with earlier results obtained by the homogeneous deformation method. The role of three-body correlations in the functional expansion is discussed, but the illustrative calculations that we present include only the Ornstein–Zernike two-body direct correlation function of the liquid, weighted by a Debye–Waller factor. The Ornstein–Zernike function can be obtained either directly from the measured liquid structure factor or by liquid structure theory in model systems. Our calculations of phonon dispersion relations and elastic constants refer to the BCC metals sodium and potassium, to a Lennard-Jones model for FCC argon, and to the classical one-component plasma crystallized in the BCC and FCC structures. The theoretical results are compared with neutron inelastic scattering and elastic constants data on sodium, potassium and argon, as well as with computer simulation data on the crystallized plasma.

1. Introduction

The theory of lattice dynamics and elastic constants of crystal is a fully developed branch of solid-state physics, starting from the very early work of Born and his co-workers (see, for example, Born and Huang [1]). The central role in the theory is played by the potential energy of the crystal as a function of the nuclear positions, which is expanded in powers of the displacements of the nuclei from the equilibrium lattice sites. The quasi-harmonic approximation can be transcended to treat anharmonic terms in the expansion either by perturbation theory (see, for example, Cowley [2, 3]) or by the self-consistent phonon approach (see, for example, Choquard [4], Glyde and Klein [5]). Anharmonicity results in both a renormalization of the phonon frequencies and a broadening of the phonons, which become increasingly important with increasing temperature.

In the present work we treat the lattice dynamics and the elastic constants of a crystal close to melting from an entirely different point of view, which gives weight to structure and leaves the role of the interatomic forces implicit. Our approach relates the renormalized phonon frequencies to the direct correlation functions of the liquid near freezing. These functions were first introduced in liquid state theory by Ornstein and Zernike [6] and, in a system obeying classical statistical mechanics, have simultaneously the meaning

0953-8984/91/509943 + 21 $03.50

of static response functions and of structural functions. The relationship is established within the density functional method by expanding the free energies of a suitably deformed crystal and of the undeformed crystal at melting around the liquid at freezing. At the simplest level of approximation the result is to allow an evaluation of the full set of phonon dispersion relations in the high-temperature crystal from the static structure factor of the liquid, weighted by a Debye–Waller factor. The fact that the liquid structure factor, in its full dependence on wave-number, contains information on the renormalized force constants in the crystal at melting is also conceptually interesting from the viewpoint of liquid state theory. While we note that we have no access in our approach to phonon broadening by anharmonicity, we may recall that in theories of liquid state dynamics the structure factor enters to determine the frequencies of density fluctuations in situations where the damping of propagating modes is high (see, for example, March and Tosi [7]).

Our work falls within a major line of development of the density functional method as applied to classical systems, which has aimed at relating properties of a crystal near melting to the structure of its liquid near freezing. The initial impulse to this development has come from the work of Ramakrishnan and Yussouff [8] on liquid–solid coexistence, leading to a wealth of theoretical results on this phase transition (for recent reviews see Rovere *et al* [9] and Baus [10]) and on the liquid–solid interface [11, 12]. It has subsequently been pointed out by Ramakrishnan [13] and in more detail by Lipkin *et al* [14] that through the application of a homogeneous deformation to the hot crystal, one may relate its elastic constants to liquid structure (see also [15–17]). In this work we shall compare the expressions for the elastic constants that we obtain from the phonon dispersion curves by the long-waves method and those obtained by the homogeneous deformation method. Ramakrishnan [13] has also pointed out that a crystal deformed by the presence of a lattice defect may be treated by similar methods, suggesting interesting possibilities for the theoretical study of defects in crystals at high temperature.

The lay-out of the paper is briefly as follows. In section 2, we present our treatment of the free energy of the deformed crystal leading to an expression for the phonon frequencies in terms of the two-body direct correlation function of the liquid, the role of higher correlations being introduced by including three-body correlations which are then discussed in some detail in the appendix. Section 3 deals with the long wavelength limit and discusses the elastic constants as well as the longitudinal plasma mode at long wavelength in the case of the classical Wigner crystal. Section 4 presents numerical results and comparisons with experimental or computer simulation data for BCC alkali metals, for a Lennard-Jones model of FCC argon, and for the crystallized plasma in both the BCC and FCC structure. Section 5 concludes the paper with a summary and some final remarks. A preliminary report of this work has already appeared in the literature [18].

2. Theory of phonon dispersion relations

We consider a monatomic classical system with an inhomogeneous single-particle density profile $n(\boldsymbol{r})$ and treat its thermodynamic functions by a functional expansion method which was originally developed by Lebowitz and Percus [19] and by Yang, Fleming and Gibbs [20]. The same method has been used in the theory of liquid–solid coexistence

(see, for example, Haymet and Oxtoby [11]). The grand thermodynamic potential Ω as a functional of $n(r)$ is given by

$$\Omega[n(r)] = F[n(r)] + \int \mathrm{d}r\, n(r)[U(r) - \mu]$$

$$= -\varphi[n(r)] + k_B T \int \mathrm{d}r\, n(r)[C(r) - 1]. \tag{1}$$

In (1) F is the Helmholtz free energy aside from the interaction of the system with the external potential $U(r)$, μ is the chemical potential, $-\varphi$ is the non-ideal contribution to the free energy arising from the interactions between the particles, and

$$C(r) = (k_B T)^{-1} \delta\varphi[n(r)]/\delta n(r). \tag{2}$$

The higher functional derivatives of φ define a hierarchy of correlation functions,

$$c(r_1, r_2) = \delta C(r_1)/\delta n(r_2) = (k_B T)^{-1} \delta^2 \varphi[n(r)]/\delta n(r_1)\delta n(r_2) \tag{3}$$

$$c^{(3)}(r_1, r_2, r_3) = \delta^2 C(r_1)/\delta n(r_2)\delta n(r_3) \tag{4}$$

etc. The functional expansion of $C(r)$ around its value C_1 in the homogeneous fluid at density n_1 thus reads

$$C(r) = C_1 + \int \mathrm{d}r' c(|r' - r|)[n(r') - n_1] + \frac{1}{2}\int\int \mathrm{d}r'\, \mathrm{d}r'' c^{(3)}(r' - r, r'' - r)[n(r') - n_1][n(r'') - n_1] + \ldots. \tag{5}$$

The correlation functions in (5) refer to the fluid at density n_1. A similar functional expansion for $\varphi[n(r)]$ leads to

$$\Omega[n(r)] = \Omega_1 - k_B T \int \mathrm{d}r[n(r) - n_1]$$

$$+ \tfrac{1}{2} k_B T \int\int \mathrm{d}r\, \mathrm{d}r' c(|r - r'|)[n(r) + n_1][n(r') - n_1]$$

$$+ \tfrac{1}{6} k_B T \int\int\int \mathrm{d}r\, \mathrm{d}r'\, \mathrm{d}r'' c^{(3)}(r' - r, r'' - r)$$

$$\times [2n(r) + n_1][n(r') - n_1][n(r'') - n_1] + \ldots \tag{6}$$

where Ω_1 is the grand potential in the fluid.

We are specifically interested in a monatomic system crystallizing in a simple Bravais lattice structure described by a set of lattice sites R_i, which is deformed by giving to each site a displacement d_i. In particular, we consider a wave of lattice displacements of the form

$$d_i = N^{-1/2} \xi_{qs} \cos(q \cdot R_i) \tag{7}$$

which is generated at constant temperature, volume and chemical potential. In (7) N is the number of lattice sites and ξ_{qs} is (aside from normalization) the eigenvector of a lattice vibration of wave-vector q and polarization index s. As such ξ_{qs} is invariant under

the transformation $q \to q + G$, where G is any reciprocal lattice vector (RLV). The density profile of the deformed crystal is given by

$$n(r) = \left\langle \sum_i \delta(r - R_i - d_i - u_i(t)) \right\rangle \tag{8}$$

where $u_i(t)$ are the atomic displacements due to thermal fluctuations and the brackets denote the statistical average. After a Fourier transform we write

$$n(r) = \frac{1}{V} \sum_k f(k) \sum_i \exp[ik \cdot (r - R_i - d_i)] \tag{9}$$

where

$$f(k) = \langle \exp[-ik \cdot u_i(t)] \rangle. \tag{10}$$

$f(k)$ describes the average spread of atomic density around each lattice site due to thermal fluctuations, that we have assumed to be unchanged by the deformation. In fact, we shall later assume this spread to be of the Gaussian type leading, for a cubic crystal, to

$$f(k) = \exp(-\tfrac{1}{6}k^2\langle u^2 \rangle) \tag{11}$$

where $\langle u^2 \rangle$ is the mean square atomic displacement from thermal fluctuations. These approximations on the role of thermal fluctuations in the density profile of the deformed crystal should be subject to further theoretical study.

By using (7) in (9), expanding the exponential up to quadratic terms in ξ_{qs} and using the relation $\Sigma_i \exp(ik \cdot R_i) = N\delta_{k,G}$, we find

$$\begin{aligned} n(r)/n_s = {} & \sum_G f(G)[1 - (1/4N)(G \cdot \xi_{qs})^2] \exp(iG \cdot r) \\ & + N^{-1/2} \sum_G f(q + G)[(q + G) \cdot \xi_{qs}] \sin[(q + G) \cdot r] \\ & - (1/4N) \sum_G f(2q + G)[(2q + G) \cdot \xi_{qs}]^2 \cos[(2q + G) \cdot r] \end{aligned} \tag{12}$$

where n_s is the average density of the crystal. The last term on the right-hand side of this equation could, for our purposes, be dropped already at this point, since it will ultimately contribute to the free energy of deformation, to quadratic terms in ξ_{qs}, only for q lying on a zone boundary ($q = G/2$). For such values of q the density profile as written in (12) includes two physically equivalent lattice waves, with wave-vectors lying at opposite points on the zone boundary, and only one of them should be counted in evaluating the free energy of deformation.

The change in grand potential accompanying the deformation follows by inserting (12) in (6) and subtracting the corresponding value of Ω for the undeformed crystal ($\xi_{qs} = 0$). With the definition

$$c(k) = n_1 \int dr\, c(r) \exp(ik \cdot r) \tag{13}$$

we find that the work done in deforming the crystal is

$$\begin{aligned} \Delta\Omega = (n_s k_B T/4n_1) \Big\{ & \sum_G f^2(q + G) c(|q + G|)[(q + G) \cdot \xi_{qs}]^2 \\ & - \sum_{G \neq 0} f^2(G) c(G)(G \cdot \xi_{qs})^2 \Big\} \end{aligned} \tag{14}$$

per particle. We have retained in (14) only the terms arising in (6) from the two-body direct correlation function. The contributions coming from three-body and higher correlations are discussed in the appendix.

$\Delta\Omega$ in (14) contains both the interaction of the deformation with the external potential causing it and the intrinsic free energy change stored in the deformed crystal. Equating $\Delta\Omega$ to $-\pi^2 M\nu_{qs}^2|\xi_{qs}|^2$, where M is the atomic mass and ν_{qs} is the frequency eigenvalue of the lattice vibration indexed by q and s, we find the expression for the dispersion relations

$$\nu_{qs}^2 = -(n_s k_B T/4\pi^2 n_1 M)\Big\{\sum_G f^2(q+G)c(|q+G|)[(q+G)\cdot\hat{\varepsilon}_{qs}]^2 - \sum_{G\neq 0} f^2(G)c(G)(G\cdot\hat{\varepsilon}_{qs})^2\Big\} \tag{15}$$

where $\hat{\varepsilon}_{qs} = \xi_{qs}/|\xi_{qs}|$ is the normalized eigenvector of the lattice vibration. The expression (15) contains both longitudinal modes ($\hat{\varepsilon}_{qs} \parallel q$) and transverse modes ($\hat{\varepsilon}_{qs} \perp q$), the latter arising from the 'Umklapp' factors $G\cdot\hat{\varepsilon}_{qs}$ in both sums over RLVs.

It is easily shown that the expression (15) for the dispersion relation is invariant under translation of q by any RLV. This property follows from the invariance of $\hat{\varepsilon}_{qs}$ under such a translation and from the fact that the sum of two RLVs is again an RLV. In all the calculations that we shall report below we have checked that (15) yields the same results along equivalent directions in the Brillouin zone and reproduces the degeneracies of phonon branches that are expected from symmetry.

The relationship of the quantities in (15) to structure is immediate for the Ornstein–Zernike function $c(k)$ which, by the classical fluctuation–dissipation theorem, is related to the liquid structure factor $S(k)$ by

$$c(k) = 1 - 1/S(k). \tag{16}$$

With regard to the function $f(k)$, on the other hand, we note that the Ramakrishnan–Yussouff theory of freezing allows one to evaluate the quantities $f^2(G)$ for the crystal at melting from the same information on liquid structure. These are the well-known Debye–Waller factors giving the intensity of the Bragg reflections from the crystal and hence have a direct structural meaning. The theory of freezing allows a test of the Gaussian approximation and an estimate of the mean square displacement $\langle u^2\rangle$ in the crystal at melting. However, in the calculations reported below we have preferred, for a more stringent test of our theoretical results, to adopt (11) for cubic crystals with values of $\langle u^2\rangle$ obtained from data on the crystal.

3. Long wavelength limit

The elastic constants follow from the dispersion relations (15) by the method of long waves, i.e. by taking the limit $q \to 0$. We consider first the case of a system composed of atoms, in which $c(q)$ tends to a constant $c(0)$ given by

$$c(0) = 1 - (n_1 k_B T K_T)^{-1} \tag{17}$$

K_T being the isothermal compressibility of the liquid. The case of the plasma, in which $c(q)$ contains a Coulomb term which diverges for $q \to 0$, will be discussed later in this section.

Considering for simplicity a cubic crystal, where $f(k)$ is isotropic, and introducing the notation $F(k) = f^2(k)$, a lengthy but straightforward calculation leads to

$$-(4\pi^2 n_1 M \nu_{qs}^2/n_s k_B T q^2) \to \Big[c(0) + \sum_{G\neq 0} F(G)c(G)\Big](\hat{q}\cdot\hat{\varepsilon}_{qs})^2 + \sum_{G\neq 0} D(G)(\hat{G}\cdot\hat{\varepsilon}_{qs})\{4(\hat{q}\cdot\hat{\varepsilon}_{qs})(\hat{G}\cdot\hat{q}) + (\hat{G}\cdot\hat{\varepsilon}_{qs})[1-(\hat{G}\cdot\hat{q})^2]\} + \sum_{G\neq 0} E(G)(\hat{G}\cdot\hat{\varepsilon}_{qs})^2(\hat{G}\cdot q)^2 \tag{18}$$

with

$$D(G) = (1/2)G[F'(G)c(G) + F(G)c'(G)] \tag{19}$$

and

$$E(G) = (1/2)G^2[F''(G)c(G) + 2F'(G)c'(G) + F(G)c''(G)]. \tag{20}$$

$\hat{G}$ and $\hat{q}$ are the unit vectors in the directions of G and q. Clearly, a dispersion behaviour of acoustic type is recovered at long waves.

Explicit expressions for the elastic constants follow from (18) by considering specific directions of wave propagation and polarization. Taking $\hat{q} = [100]$ and $\hat{\varepsilon}_{qs} = [001]$ we find

$$c_{44} = -\frac{n_s^2 k_B T}{n_1}\sum_{G\neq 0}\left[D(G)\left(\frac{1}{3} - \frac{G_x^2 G_y^2}{G^4}\right) + E(G)\frac{G_x^2 G_y^2}{G^4}\right] \tag{21}$$

whereas from $\hat{q} = [100]$ and $\hat{\varepsilon}_{qs} = [100]$ we find

$$c_{11} = -\frac{n_s^2 k_B T}{n_1}\left\{\left[c(0) + \sum_{G\neq 0} F(G)c(G)\right] + \sum_{G\neq 0}\left[D(G)\left(\frac{5}{3} - \frac{G_x^4}{G^4}\right) + E(G)\frac{G_x^4}{G^4}\right]\right. \tag{22}$$

Finally, considering a wave which propagates along the [110] direction with polarization in the $[1\bar{1}0]$ direction we find the elastic constant $(c_{11} - c_{12})/2$,

$$\tfrac{1}{2}(c_{11} - c_{12}) = -\frac{n_s^2 k_B T}{n_1}\sum_{G\neq 0}\left[D(G)\left(\frac{1}{6} + \frac{3}{2}\frac{G_x^2 G_y^2}{G^4}\right) + E(G)\left(\frac{1}{6} - \frac{3}{2}\frac{G_x^2 G_y^2}{G^4}\right)\right] \tag{23}$$

and hence

$$c_{12} = -\frac{n_s^2 k_B T}{n_1}\left\{\left[c(0) + \sum_{G\neq 0} F(G)c(G)\right] + \sum_{G\neq 0}\left[D(G)\left(1 - \frac{G_x^2 G_y^2}{G^4}\right) + E(G)\frac{G_x^2 G_y^2}{G^4}\right]\right\}. \tag{24}$$

In deriving these equations, account has been taken of cubic symmetry in the summations over the RLVs within each star.

Before comparing the foregoing results with those obtained by the homogeneous deformation method, we pause to discuss the special case of long wavelength vibrations in the crystallized plasma. In this system the limiting behaviour (17) is replaced by

$$c(q \to 0) = -(4\pi n_1 e^2)/(k_B T q^2) + \text{constant} \tag{25}$$

and hence it is immediately seen from (18) that the longitudinal mode tends to the plasma frequency [21]

$$\omega_p = (4\pi n_s e^2/M)^{1/2}. \tag{26}$$

The constant in (25) enters to determine a quadratic dispersion of the optic mode as one moves away from the zone centre. The transverse modes are instead acoustic near the zone centre, the elastic constants c_{44} and $(c_{11} - c_{12})/2$ still being given by (21) and (23).

We turn next to the homogeneous deformation method for the evaluation of the elastic constants. We follow the treatment already given by Lipkin *et al* [14]. A homogeneous strain is applied to the crystal at constant temperature, volume and chemical potential. The density profile $n(\boldsymbol{r})$ of the deformed crystal is obtained by noting that the RLVs change from $\boldsymbol{G}$ to $\boldsymbol{G} \cdot (\mathbf{1} + \varepsilon)^{-1}$, where ε is the strain tensor. From (12) at $\xi_{qs} = 0$ one has

$$n(\boldsymbol{r})/n_s = 1 + \sum_{G \neq 0} f(\boldsymbol{G} \cdot (\mathbf{1} + \varepsilon)^{-1}) \exp[i\boldsymbol{G} \cdot (\mathbf{1} + \varepsilon)^{-1} \cdot \boldsymbol{r}] \tag{27}$$

and hence from (6) the work done in deforming the crystal is

$$\Delta\Omega = (n_s^2 k_B T)/(2n_1^2) \sum_{G \neq 0} [c(|\boldsymbol{G} \cdot (\mathbf{1} + \varepsilon)^{-1}|) f^2(\boldsymbol{G} \cdot (\mathbf{1} + \varepsilon)^{-1}) - c(G) f^2(\boldsymbol{G})] \tag{28}$$

including again only the terms from two-body correlations. Expansion of (28) in powers of the components of the strain tensor and comparison of the quadratic terms with the well-known results of elasticity theory yield the three elastic constants for a cubic crystal.

It is immediately evident that the expansion leads to expressions for the elastic constants involving the functions $D(G)$ and $E(G)$ defined in (19) and (20), while the contributions coming in the long-waves method from the first term on the right-hand side of (18) are missing in the homogeneous deformation method. We have seen above that, in the long-waves method, one of these contributions is responsible for the plasma-mode behaviour of the longitudinal vibration in the classical Wigner crystal. Similarly, for systems where (17) is applicable, the $c(0)$ terms in (22) and (24) contribute a term $n_s^2/(n_1^2 K_T)$ to the bulk modulus of the crystal from the compressibility K_T of the liquid. There is, therefore, an obvious discrepancy between the results obtained for the elastic constants in the two methods.

The expansion of (28) leads to

$$c_{44} = -\frac{n_s^2 k_B T}{n_1} \sum_{G \neq 0} \left[D(G)\left(\frac{1}{2} - \frac{G_x^2 G_y^2}{G^4}\right) + E(G)\frac{G_x^2 G_y^2}{G^4} \right] \tag{29}$$

$$c_{11} = -\frac{n_s^2 k_B T}{n_1} \sum_{G \neq 0} \left[D(G)\left(1 - \frac{G_x^4}{G^4}\right) + E(G)\frac{G_x^4}{G^4} \right] \tag{30}$$

and

$$c_{12} = -(n_s^2 k_B T/n_1) \sum_{G \neq 0} [-D(G) + E(G)](G_x^2 G_y^2/G^4). \tag{31}$$

On comparison with (21)–(24) one notices that, whereas there is agreement between

the results of the two methods in the terms determined by $E(G)$, there are additional discrepancies arising from the terms containing $D(G)$.

As is well known from a number of previous instances in the literature, discrepancies between the long-waves method and the homogeneous deformation method commonly arise from the use of truncated expansions. We shall examine in sections 4.2 and 4.3 below the numerical importance of the above discrepancies between the two methods for the calculation of elastic constant. We also note that in their treatment of (28) Lipkin *et al* [14] omitted the dependence of f^2 on strain and set $c'(G) = 0$. In this case $D(G) = 0$ and the expressions (29)–(31) show that the calculated elastic constants c_{12} and c_{44} would satisfy the Cauchy relation $c_{12} = c_{44}$. We shall illustrate the numerical consequences of these approximations in sections 4.2 and 4.3.

4. Numerical results

4.1. Dispersion curves and elastic constants of sodium and potassium

In our calculations of the phonon dispersion relations for the BCC alkali metals Na and K, we use values of $c(k)$ obtained directly from the measured values of the structure factor $S(k)$ of the liquid near freezing, from x-ray diffraction experiments [22] and from neutron diffraction experiments [23]. The Debye–Waller factors in (15) are crucial in ensuring convergence of the summations over RLVs. In the case of Na, where the $S(k)$ data extend over a more limited range of wave-number (covering 11 stars of RLVs in the x-ray data and 15 stars in the neutron data), we obtain convergence within a few parts in 10^3. For the Debye–Waller factors we have used the Gaussian approximation (11), taking the mean square displacement $\langle u^2 \rangle$ at the melting temperature T_m (or equivalently the Lindemann parameter $L = (\langle u^2 \rangle / d^2)^{1/2}$ with d the first neighbour distance) from evaluations based on phonon frequency spectra constructed from neutron inelastic scattering data [24]. For both Na ($T_m = 371$ K) and K ($T_m = 336$ K) we have taken $L = 0.15$, the primary data being those of Woods *et al* [25] on Na at 90 K and those of Cowley *et al* [26] and of Dolling and Meyer [27] on K at 9 K and below. It is worth pointing out that a recent calculation of the liquid–solid transition of the alkali metals within the Ramakrishnan–Yussouff theory has found that the Gaussian approximation is quite good (although the theory has problems in dealing with the Debye–Waller factor at the (200) star) and has estimated $L \approx 0.15$ [28].

Our results for the phonon dispersion relations of Na and K at melting are reported in figures 1 and 2, respectively. In these and the following figures, the curves referring to some propagation directions are repeated to show the degeneracies at the zone boundaries with other branches. The results for Na are compared in figure 1 with the data of Woods *et al* [25] at 90 K and with those reported by Glyde and Taylor [29] at 296 K. The results for K are compared in figure 2 with the data of Cowley *et al* [26] at 9 K and with those of Buyers and Cowley [30] at 299 K. It is evident that for both metals there is substantial agreement between the theoretical results obtained with the two sets of structure factor data, and also that our results have the general shapes of the measured dispersion curves. The quantitative agreement with the high temperature data is quite good, especially for the transverse modes in the [00ξ] and [$\xi\xi$0] directions and for the F_1 branch in the [$\xi\xi\xi$] direction. However, the observed lowering of the longitudinal branch in the [$\xi\xi$0] direction with increasing temperature is not reproduced. The general effect of an increase in temperature is a downward shift of the phonon frequencies,

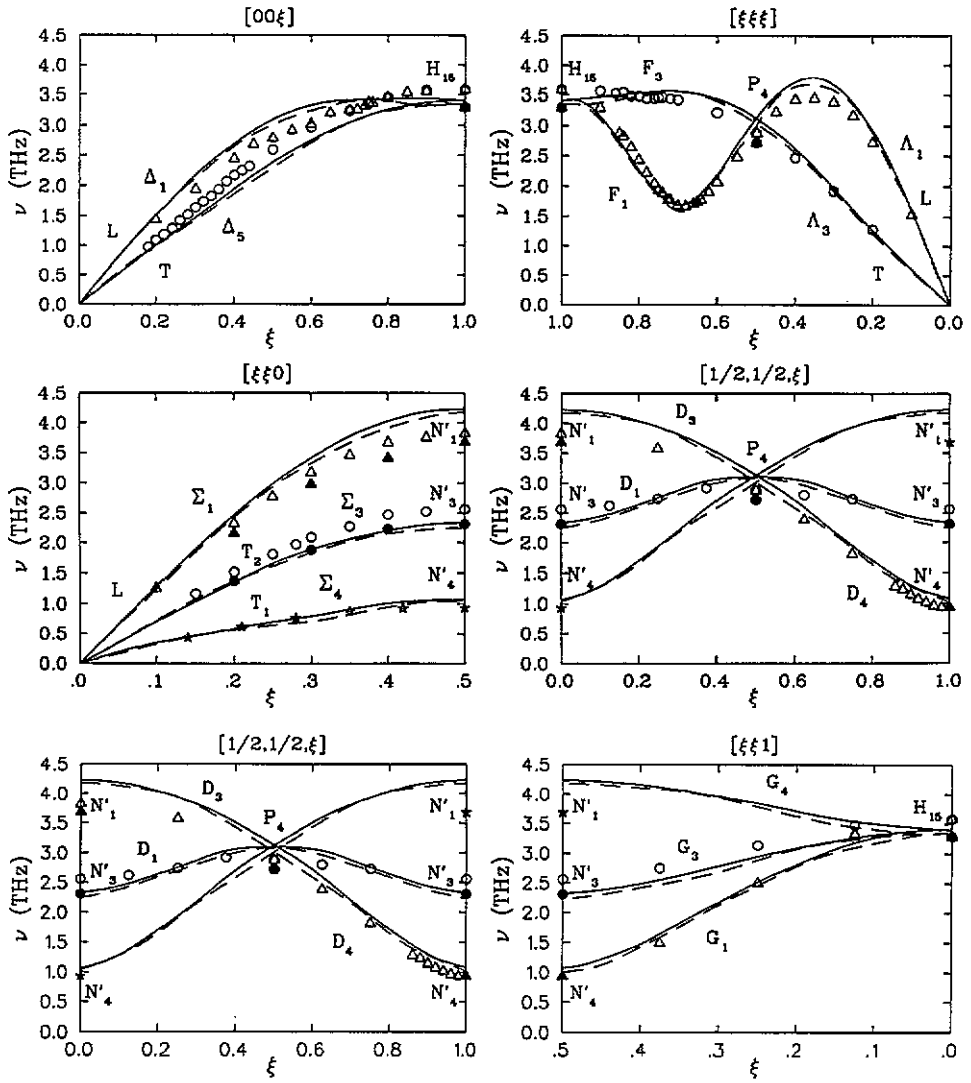

Figure 1. Calculated dispersion relations for phonons in Na at melting, from liquid structure data obtained by x-ray diffraction (full curves) and neutron diffraction (broken curves), compared with those obtained from neutron inelastic scattering experiments at 90 K by Woods *et al* [25] (open circles, triangles and stars) and at 296 K as reported by Glyde and Taylor [29] (full circles, triangles and stars). The direction of the wave-vector $\boldsymbol{q}$, with components in units of $\pi\sqrt{3}/d$, is indicated at the top of each graph.

as was calculated for K by Buyers and Cowley [30] in a perturbative treatment of anharmonicity and for Na by Glyde and Taylor [29] in a self-consistent phonon approach. The latter authors stressed, however, that the T_1 [$\xi\xi$0] branch is an exception to this broad rule.

The use of measured values for the two-body correlations has instead limited usefulness in the calculation of elastic constants. We have found it impossible to derive from the liquid structure factor data the values of $c'(G)$ and $c''(G)$ needed to evaluate $D(G)$

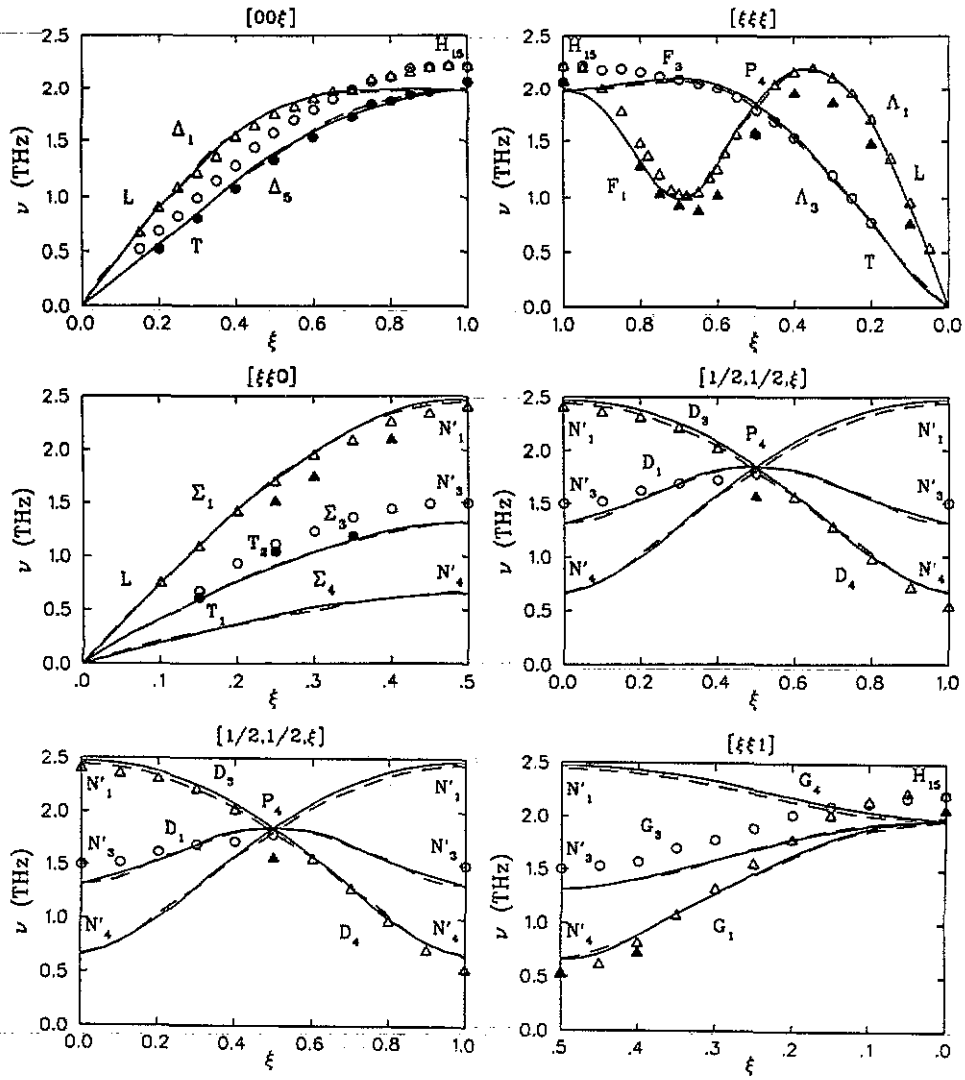

Figure 2. Calculated dispersion relations for phonons in K at melting, from liquid structure data obtained by x-ray diffraction (full curves) and neutron diffraction (broken curves), compared with those obtained from neutron inelastic scattering experiments at 9 K by Cowley *et al* [26] (open circles and triangles) and at 299 K by Buyers and Cowley [30] (full circles and triangles). The direction of the wave-vector q, with components in units of $\pi\sqrt{3}/d$, is indicated at the top of each graph.

and $E(G)$ with the necessary accuracy. One may, however, still evaluate the elastic constants in the long-waves method from the slopes of the calculated dispersion curves near the zone centre. The results that we estimate for the elastic constants of Na and K at melting from the slopes of the calculated dispersion curves in figures 1 and 2 are shown in table 1, in comparison with the adiabatic elastic constants measured for Na at 368 K [31] and for K at 336 K [32] by ultrasonic techniques. It is evident that the magnitude of the elastic constants is well reproduced in both systems, though there is some tendency

Table 1. Elastic constants of Na and K at melting (in GPa), calculated graphically by the long-waves method from primary data of x-ray or neutron diffraction on the melt and compared with experimental values of Fritsch *et al* [31, 32].

	X-ray	Neutron	Experiment
Na c_{11}	7.6	8.2	7.35 ± 0.12
c_{12}	6.9	7.3	6.13 ± 0.04
c_{44}	4.2	3.9	3.79 ± 0.04
K c_{11}	4.0	4.1	3.50 ± 0.02
c_{12}	3.5	3.3	3.08 ± 0.08
c_{44}	2.0	2.3	1.68 ± 0.02

to overestimate them. It is particularly satisfactory that the theoretical results account for the large deviation from the Cauchy relation between c_{12} and c_{44}.

4.2. Dispersion curves and elastic constants of argon

In our calculations on argon as an example of FCC crystals, we have adopted a Lennard-Jones model potential in order to carry out accurate liquid structure calculations, which enable us to test the various approaches to the elastic constants that we have presented in section 3. The parameters of the Lennard-Jones potential are taken from the work of Moleko and Glyde [33]. The liquid structure is evaluated by the integral equations technique of Zerah and Hansen [34], which is known from a number of previous calculations on various fluid systems to yield very accurate results. In particular, the approach that we have followed ensures thermodynamic self-consistency on the value of the isothermal compressibility of the liquid as obtained from the virial theorem and from thermodynamic fluctuation theory, yielding $c(0) = -18.1$ against the experimental value $c(0) = -18.9$ [35]. The range of wave-number in our calculation of $S(k)$ covers 26 stars of RLVs, ensuring convergence of the sums in (15) to a few parts in 10^4. We have taken the Lindemann parameter $L = 0.145$ from Monte Carlo simulation data on essentially the same Lennard-Jones system near the triple point [36].

Our results for the phonon dispersion relations of argon at melting ($T_m = 83.78$ K) are shown in figure 3. They are compared with those reported at 10 K and at 82 K by Fujii *et al* [37] from neutron inelastic scattering experiments on samples of isotopically pure ^{36}Ar, after rescaling the frequencies by the factor $(36/39.948)^{1/2}$. The calculated dispersion curves again have the correct general shapes and satisfactorily account for the observed lowering of phonon frequencies with increasing temperature. In the experiments at 82 K the observed phonon profiles were too broad and weak to allow reasonable estimates of the phonon frequencies, except over a limited range of wave-number [37]. The phonon frequencies and widths obtained in a more limited neutron inelastic scattering study of argon at 77 K [38] have been discussed theoretically by Klein *et al* [39] in a perturbative treatment of anharmonicity. They found good agreement with the data, except for the transverse [00ξ] branch.

Table 2 reports the values of the elastic contants of argon at melting as calculated by various methods and compares them with the data of Gewurtz and Stoicheff [40] on adiabatic elastic constants at 82.3 K from Brillouin scattering experiments. Evidently, the long-waves method gives, for this system, results that are quite reasonable, though

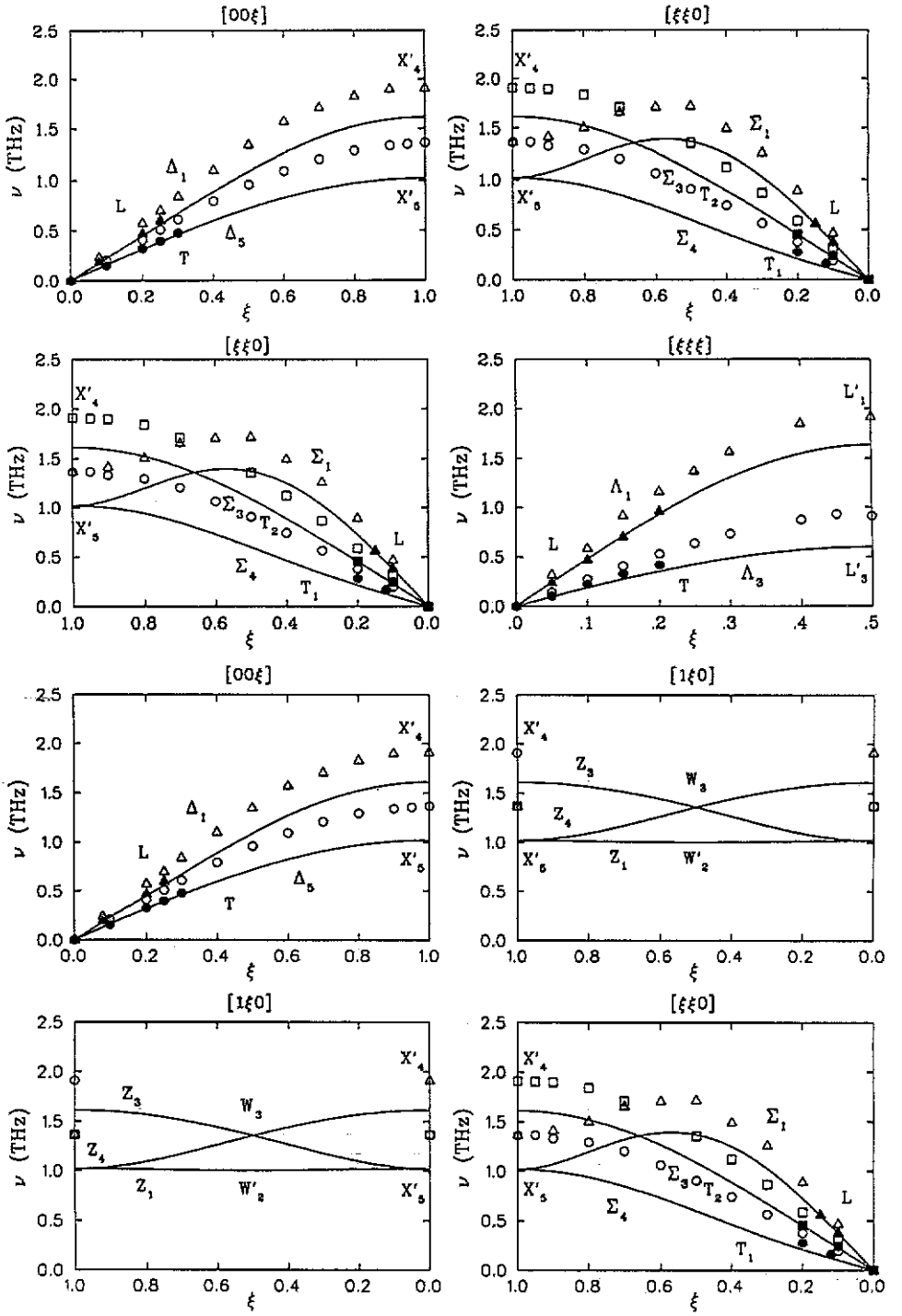

Figure 3. Calculated dispersion relations for phonons in argon at melting, from liquid structure calculations in a Lennard–Jones model, compared with those obtained from neutron inelastic scattering experiments at 10 K (open circles, squares and triangles) and at 82 K (full circles, squares and triangles) by Fujii *et al* [37]. The direction of the wave-vector q, with components in units of $\pi\sqrt{2}/d$, is indicated at the top of each graph.

Table 2. Elastic constants of a Lennard-Jones model of argon at melting (in GPa), calculated from (a) the slopes of the dispersion curves; (b) the long-waves method formulae; (c) the homogeneous deformation method formulae, and (d) the formulae of Lipkin *et al* [14]. The experimental values are from Gewurtz and Stoicheff [40].

	(a)	(b)	(c)	(d)	Experiment
c_{11}	2.44	2.43	1.76	1.71	2.38 ± 0.04
c_{12}	1.92	1.93	1.15	1.08	1.56 ± 0.03
c_{44}	1.24	1.26	1.31	1.08	1.12 ± 0.03

not fully quantitative. Its performance in relation to the deviation from the Cauchy relation is again quite satisfactory. We note that the measured elastic constants of argon drop by almost a factor of two in going from 10 K to 82.3 K [37, 40]. Such a drop arises to a large extent from the thermal expansion of the crystal [41] and has been accounted for in simulation work on the high-temperature crystal [42].

4.3. Dispersion curves and elastic constants of the classical Wigner crystal in the BCC and FCC structures

The classical one-component plasma, which is a model system composed of identical point-like charges on a uniform neutralizing background, is characterized by its coupling strength parameter $\Gamma = e^2/ak_BT$ with $a = (4\pi n/3)^{-1/3}$. The fluid phase is known from computer simulation work to crystallize into the BCC structure, the latest value for the coupling strength at the phase transition being $\Gamma = 178$ [43]. A transition of the supercooled fluid into the FCC structure has also been reported at $\Gamma = 192$ [44, 43].

In our calculations we have adopted the generalized mean spherical approximation [45] to evaluate the structure factor of the fluid. This yields analytic results for $c(k)$ that incorporate the expression of the internal energy of the fluid as a function of Γ from simulation [43]. The results are thermodynamically self-consistent, and are known to be highly accurate by comparison with simulation data on the structure of the fluid. We have used the analytic expression for $c(k)$ to evaluate analytically the derivatives $c'(G)$ and $c''(G)$ entering (19) and (20) and have checked the results by independent numerical calculations. The calculations of phonon dispersion relations and elastic constants have been carried out with the fluid taken both at $\Gamma = 178$ (crystallization into BCC structure) and at $\Gamma = 192$ (crystallization into FCC structure). In the former case we have taken the Lindemann parameter $L = 0.16$ from Monte Carlo simulation data [46], while in the latter we have calculated $L = 0.22$ from the harmonic expression for the mean square displacement [47] using the frequencies of lattice vibrations in the FCC structure given by Helfer *et al* [44].

Our results for the phonon dispersion curves of the classical Wigner crystal in the BCC and FCC structures at melting are shown in figures 4 and 5, respectively. We have found that the $T_1[\xi\xi 0]$ mode in the FCC structure becomes unstable near the zone centre, and in this case we show in figure 5 the modulus of the calculated frequencies with a negative sign. The calculated dispersion curves are compared with the results of the harmonic calculations by Carr [48] and Clark [49] on the BCC structure and by Helfer *et al* [44] on the FCC structure, to indicate that the general shapes of the various dispersion branches are reproduced. We have been unable to find in the literature either simulation

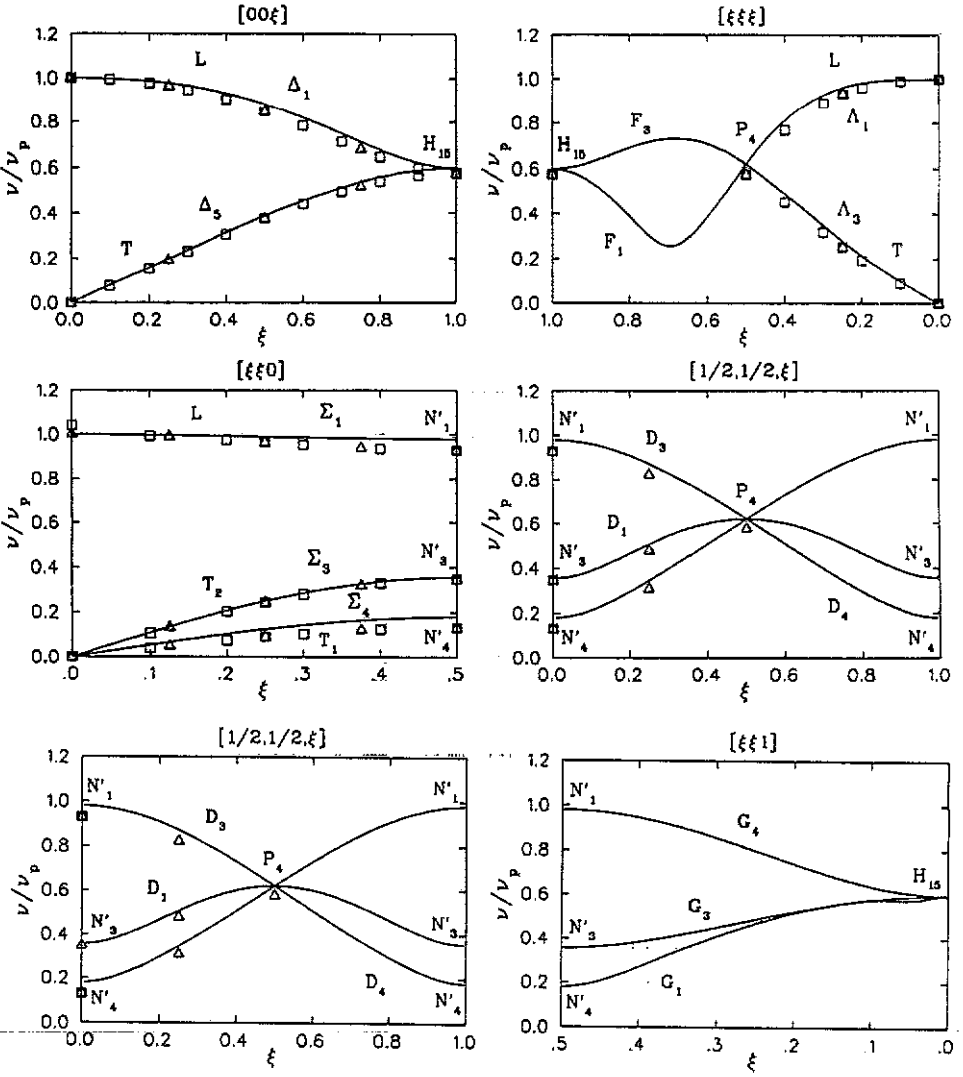

Figure 4. Calculated dispersion relations for the classical Wigner crystal in the BCC structure at $\Gamma = 178$, compared with the results of harmonic calculations by Carr [48] (triangles) and by Clark [49] (squares). The frequencies are in units of the plasma frequency ν_p and the direction of the wave-vector q, with components in units of $\pi\sqrt{3}/d$, is indicated at the top of each graph.

data or anharmonic calculations on the lattice dynamics of the classical Wigner crystal at finite Γ. Kugler [50] has shown that the dispersion curves in the harmonic approximation are the same for a classical and a quantal Wigner crystal and has proceeded to evaluate the effects of anharmonicity in the latter case, finding a general lowering of the eigenfrequencies with decreasing coupling strength. He has also discussed the Kohn sum rule,

$$\sum_s \omega_{qs}^2 = \omega_p^2 \tag{32}$$

pointing out that its validity is restricted to the harmonic approximation and showing

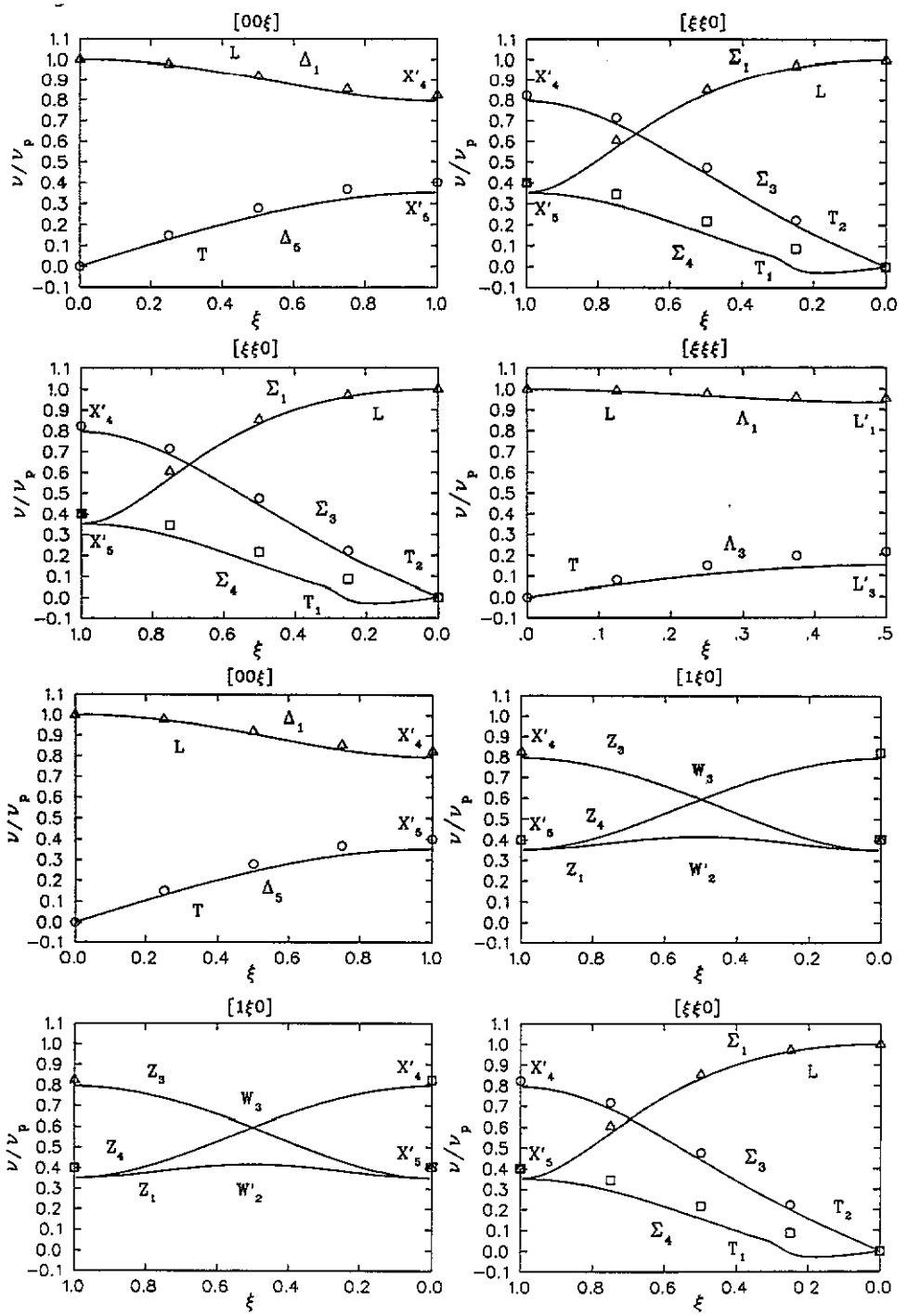

Figure 5. Calculated dispersion relations for the classical Wigner crystal in the FCC structure at $\Gamma = 192$, compared with the results of harmonic calculations by Helfer *et al* [44] (circles, squares and triangles). For the $T_1[\xi\xi 0]$ mode near the zone centre, where it is found in our calculations to be unstable, we report the modulus of the calculated frequencies with a negative sign. The frequencies are in units of the plasma frequency ν_p and the direction of the wave-vector q, with components in units of $\pi\sqrt{2}/d$, is indicated at the top of each graph.

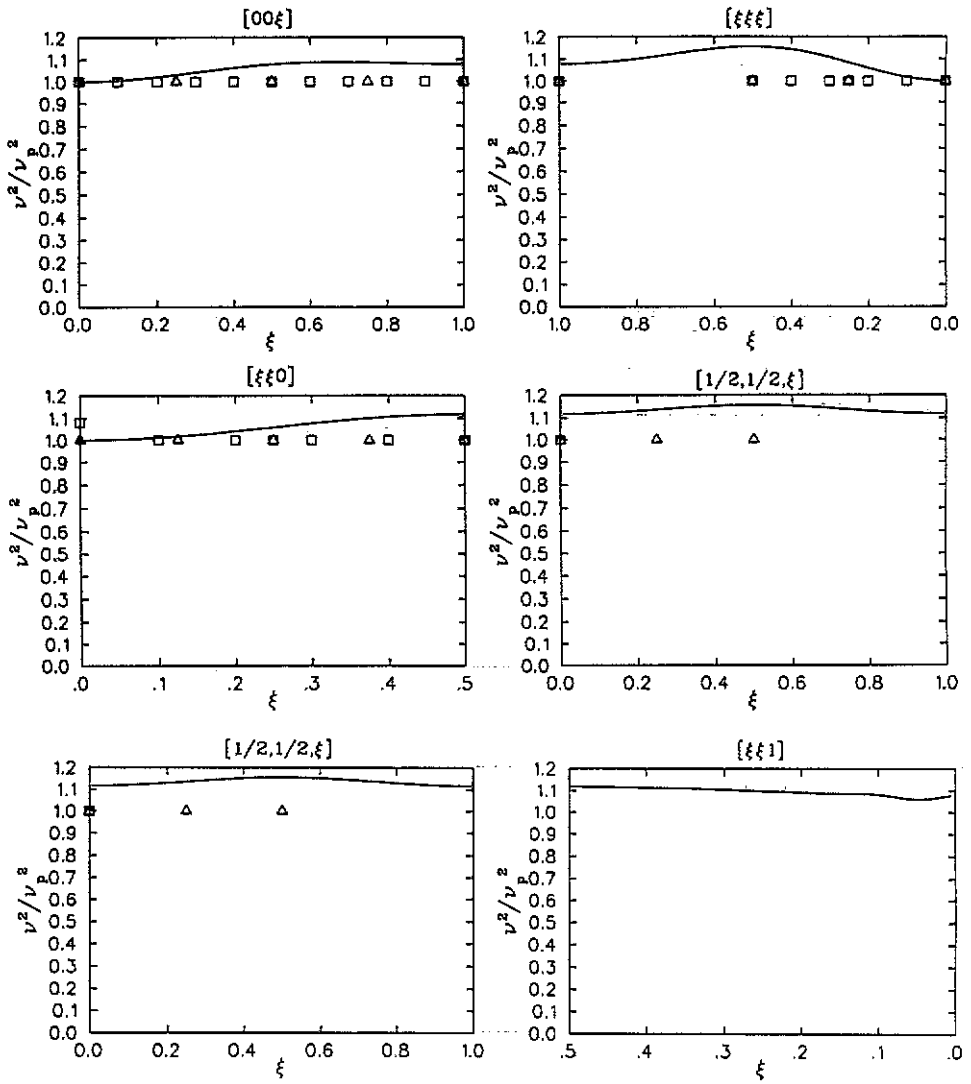

Figure 6. Calculated deviations from the Kohn sum rule in the classical Wigner crystal in the BCC structure at $\Gamma = 178$. Our results for $\Sigma_s \omega_{qs}^2$ (curves) are compared with the results obtained by Carr [48] (triangles) and by Clark [49] (squares) in the harmonic approximation.

that the sum of the squared eigenfrequencies over polarizations is lowered below ω_p^2 by anharmonicity in the quantal case. In our calculations on the classical Wigner crystal we find that this is the case only for the FCC structure, as is shown in figures 6 and 7.

Turning to the long-wavelength limit, the dispersion relation of longitudinal modes near the zone centre can be written

$$\omega_{qL} \to \omega_p + \tfrac{1}{2}\alpha_q q^2. \tag{33}$$

For example, in the [00ξ] direction we find (in units of $\omega_p d^2/\pi^2$) $\alpha = -0.2$ for the BCC structure at $\Gamma = 178$ and $\alpha = -0.4$ for the FCC structure at $\Gamma = 192$. The elastic constants

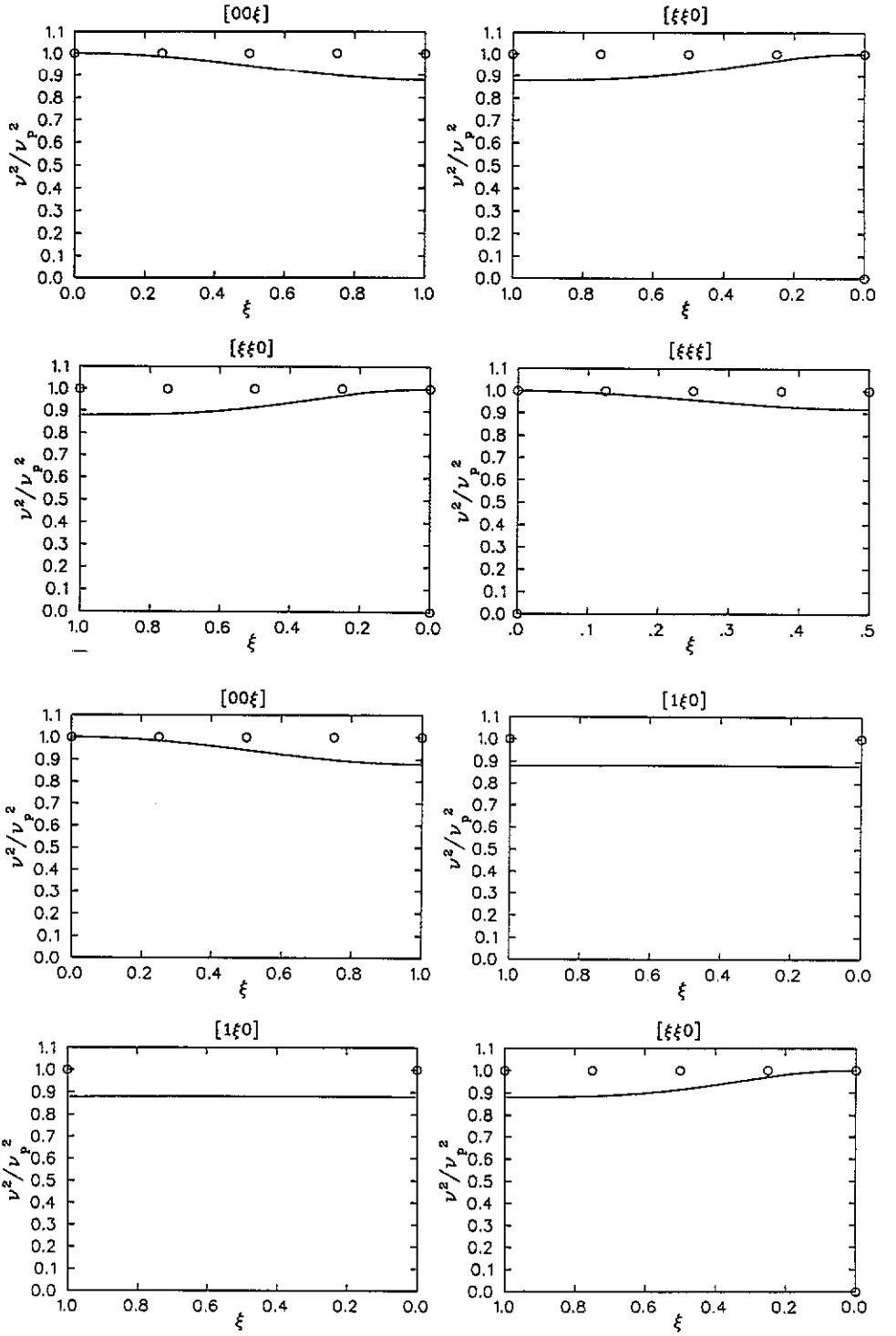

Figure 7. Calculated deviations from the Kohn sum rule in the classical Wigner crystal in the FCC structure at $\Gamma = 192$. Our results for $\Sigma_s \omega_{qs}^2$ (curves) are compared with the results obtained by Helfer *et al* [44] (circles) in the harmonic approximation.

Table 3. Elastic constants of a classical Wigner crystal in the BCC structure at $\Gamma = 178$ and in the FCC structure at $\Gamma = 192$ (in units of ne^2/a), calculated from (a) the slopes of the dispersion curves; (b) the long-waves method formulae; (c) the homogeneous deformation method formulae; and (d) the formulae of Lipkin *et al* [14]. The computer simulation values are from Ogata and Ichimaru [51] and refer to $\Gamma = 200$ for the BCC structure and to $\Gamma = \infty$ for the FCC structure.

	(a)	(b)	(c)	(d)	Simulation
BCC $(c_{11} - c_{12})/2$	4.60×10^{-2}	4.74×10^{-2}	4.90×10^{-2}	3.57×10^{-2}	1.9×10^{-2}
c_{44}	0.19	0.19	0.19	0.18	0.12
FCC $(c_{11} - c_{12})/2$	-1.17×10^{-2}	-1.26×10^{-2}	-8.35×10^{-3}	6.44×10^{-3}	2.066×10^{-2}
c_{44}	0.14	0.14	0.14	0.12	0.1852

$(c_{11} - c_{12})/2$ and c_{44} calculated by various methods for the two structures at their respective melting points are reported in table 3 and compared with recent simulation data of Ogata and Ichimaru [51] on the BCC structure at $\Gamma = 200$ and on the FCC structure at $\Gamma = \infty$. All the theoretical results reproduce the basic property that the Wigner crystal is very soft against the shear deformation described by $(c_{11} - c_{12})/2$ and much stiffer against the shear deformation described by c_{44}. As already noted, in fact we find that in the FCC structure at melting the crystal is unstable against the former deformation (except when we use the original formulae of Lipkin *et al* [14]). Quantitative comparison of the calculated elastic constants with the available data shows that the quality of the present theoretical results is considerably worse than we have found to be the case for argon in table 2. This may be a consequence of a more important role of three-body (and possibly higher) microscopic correlations in the classical plasma, as was found in the treatment of its liquid–solid transition by the Ramakrishnan–Yussouff theory (see, for example, [9]).

5. Summary and concluding remarks

We have presented a new method to evaluate the phonon dispersion relations and the elastic constants of a crystal near melting, which relates them to the direct correlation functions of its liquid near freezing with weights given by Debye–Waller factors. The main approximations leading to physically transparent and easily calculable expressions are (i) the treatment of thermal fluctuations in the crystal deformed by a wave of lattice displacements, which are taken into account through Debye–Waller factors obtained from the undeformed crystal, and (ii) the truncation of the functional expansion at two-body correlation terms. Both these aspects of the theory that we have presented could be improved: the first through a variational treatment of on-site density profiles in the deformed crystal, and the second by taking advantage of progress in the theory of liquid–solid coexistence, as we have indicated in our brief discussion of higher correlations in the appendix.

We have illustrated our theoretical results at the present level of approximation by calculations on several BCC and FCC crystals at melting, using either directly measured input for the two-body correlation function or the results of highly accurate liquid structure theories on model potentials. Although the numerical results that we have

obtained are not fully quantitative, they mostly reproduce the known trends and agree with the available data at a semi-quantitative level.

Acknowledgments

We acknowledge the sponsorship and financial support of the Ministero dell'Università e della Ricerca Scientifica e Tecnologica of Italy through the Consorzio Interuniversitario Nazionale di Fisica della Materia (CINFM). We are grateful to Dr G Pastore for providing the computer programmes needed for the liquid structure calculations. One of us (MF) wishes to thank Professor Abdus Salam, the International Atomic Energy Agency and UNESCO for hospitality at the International Centre for Theoretical Physics in Trieste under a Fellowship granted by CINFM.

Appendix. Contributions from three-body correlations

In deriving the contributions to the work of deformation which arise from the three-body correlation functions in (6), use is made of the symmetry property [52]

$$c^{(3)}(\boldsymbol{k}_1, \boldsymbol{k}_2) = c^{(3)}(\boldsymbol{k}_2, \boldsymbol{k}_1) = c^{(3)}(\boldsymbol{k}_1, -\boldsymbol{k}_1 - \boldsymbol{k}_2) \tag{A1}$$

and of the sum rule

$$\sum_{\boldsymbol{k}_1,\boldsymbol{k}_2} f(\boldsymbol{k}_1)f(\boldsymbol{k}_2)f(\boldsymbol{k}_1 + \boldsymbol{k}_2)c^{(3)}(\boldsymbol{k}_1, \boldsymbol{k}_2)(\boldsymbol{k}_1 \cdot \xi_{qs})^2$$

$$= -2 \sum_{\boldsymbol{k}_1,\boldsymbol{k}_2} f(\boldsymbol{k}_1)f(\boldsymbol{k}_2)f(\boldsymbol{k}_1 + \boldsymbol{k}_2)c^{(3)}(\boldsymbol{k}_1, \boldsymbol{k}_2)(\boldsymbol{k}_1 \cdot \xi_{qs})(\boldsymbol{k}_2 \cdot \xi_{qs}) \tag{A2}$$

which is easily proven from (A1) under the condition $f(\boldsymbol{k}) = f(-\boldsymbol{k})$. We have defined

$$c^{(3)}(\boldsymbol{k}_1, \boldsymbol{k}_2) = n_1^2 \int\int \mathrm{d}\boldsymbol{r}_{12}\, \mathrm{d}\boldsymbol{r}_{13} c^{(3)}(\boldsymbol{r}_{12}, \boldsymbol{r}_{13}) \exp[\mathrm{i}(\boldsymbol{k}_1 \cdot \boldsymbol{r}_{12} + \boldsymbol{k}_2 \cdot \boldsymbol{r}_{13})]. \tag{A3}$$

The full expression for $\Delta\Omega$ is

$$\Delta\Omega = \frac{n_s k_B T}{4n_1} \left\{ \sum_{\boldsymbol{G}} A(\boldsymbol{q} + \boldsymbol{G})[(\boldsymbol{q} + \boldsymbol{G}) \cdot \xi_{qs}]^2 - \sum_{\boldsymbol{G} \neq 0} A(\boldsymbol{G})(\boldsymbol{G} \cdot \xi_{qs})^2 \right\} + \Delta\Omega_m \tag{A4}$$

where

$$A(\boldsymbol{q} + \boldsymbol{G}) = f^2(\boldsymbol{q} + \boldsymbol{G})[c(|\boldsymbol{q} + \boldsymbol{G}|) + (1 + 2\eta)c^{(3)}(\boldsymbol{q} + \boldsymbol{G}, 0)] \tag{A5}$$

with $\eta = (n_s - n_1)/n_1$, and

$$\Delta\Omega_m = \frac{n_s^2 k_B T}{n_1^2} \sum_{\boldsymbol{G} \neq 0} B(\boldsymbol{q}, \boldsymbol{G})(\boldsymbol{q} \cdot \xi_{qs})[(\boldsymbol{q} + \boldsymbol{G}) \cdot \xi_{qs}]$$

$$+ \frac{n_s^2 k_B T}{4n_1^2} \sum_{\boldsymbol{G}_1 \neq 0} \sum_{\boldsymbol{G}_2 \neq 0, -\boldsymbol{G}_1} \{2B(\boldsymbol{G}_1, \boldsymbol{q} + \boldsymbol{G}_2)[(\boldsymbol{q} + \boldsymbol{G}_2) \cdot \xi_{qs}]$$

$$\times [(\boldsymbol{q} + \boldsymbol{G}_1 + \boldsymbol{G}_2) \cdot \xi_{qs}] - B(\boldsymbol{G}_1, \boldsymbol{G}_2)(\boldsymbol{G}_1 \cdot \xi_{qs})^2\} \tag{A6}$$

where

$$B(G_1, q + G_2) = f(G_1)f(q + G_2)f(q + G_1 + G_2)c^{(3)}(G_1, q + G_2). \tag{A7}$$

In the first term on the right-hand side of (A4) the three-body terms enter as corrections to the two-body terms from the intrinsic density dependence of $c(r)$, since

$$c^{(3)}(k, 0) = n_1^2(\partial[c(k)/n_1]/\partial n_1. \tag{A8}$$

Similar corrections enter the expression for the free energy difference between solid and liquid in the theory of freezing [11] and have been taken into account (approximately, although to infinite order in the functional expansion) in extensions of the low-order theory such as the weighted density approximation of Curtin and Ashcroft [53] (see also Curtin [54]). The implication is that such corrections could be approximately included in the dispersion relation (15) by using $c(k)$ at a suitably chosen average density rather than at the density n_1 of the liquid at freezing.

The terms collected in (A6) describe instead genuinely microscopic effects of three-body correlations. Again, a weighted density approximation takes some account of them in the theory of freezing. Schemes to estimate these microscopic couplings have been examined in the recent literature for model liquids of soft spheres [52] and of hard spheres [55]. From the experience gained in calculations on the liquid–solid transition, one should be prepared to expect important contributions from such terms in specific systems, an obvious example being the case of systems with a strong angular dependence of the interatomic forces.

The last point that we wish to make here concerns the behaviour of the three-body correlation contributions in the long wavelength limit. It is a lengthy, but straightforward calculation to show that in the limit $q \to 0$ all the three-body terms in (A4) lead to terms in ν_{qs}^2 which are of order q^2, including the case of the longitudinal optic mode in the crystallized plasma. The expression for the three-body contributions to the elastic constants and to the dispersion of the optic mode in the plasma are too lengthy to be given here, but will be available elsewhere [56].

References

[1] Born M and Huang K 1954 *Dynamical Theory of Crystal Lattices* (Oxford: University Press)
[2] Cowley R A 1963 *Adv. Phys.* **12** 421
[3] Cowley R A 1968 *Rept. Progr. Phys.* **31** 123
[4] Choquard P F 1967 *The Anharmonic Crystal* (New York: Benjamin)
[5] Glyde H R and Klein M L 1971 *Crit. Rev. Solid State Sci.* **2** 181
[6] Ornstein L S and Zernike F 1914 *Proc. Acad. Sci. Amsterdam* **17** 793
[7] March N H and Tosi M P 1976 *Atomic Dynamics in Liquids* (London: Macmillan)
[8] Ramakrishnan T V and Yussouff M 1979 *Phys. Rev.* B **19** 2775
[9] Rovere M, Senatore G and Tosi M P 1989 *Progress on Electron Properties of Solids*, ed E Doni, R Girlanda, G Pastori Parravicini and A Quattropani (Dordrecht: Kluwer) p 221
[10] Baus M 1990 *J. Phys.: Condens. Matter* **2** 2111
[11] Haymet A D J and Oxtoby D W 1981 *J. Chem. Phys.* **74** 2559
[12] Harrowell P and Oxtoby D W 1984 *J. Chem. Phys.* **80** 1639
[13] Ramakrishnan T V 1984 *Pramana* **22** 365
[14] Lipkin M D, Rice S A and Mohanty U 1985 *J. Chem. Phys.* **82** 472
[15] Jaric M V and Mohanty U 1987 *Phys. Rev. Lett.* **58** 230
[16] Velasco E and Tarazona P 1987 *Phys. Rev.* A **36** 979
[17] Jaric M V and Mohanty U 1988 *Phys. Rev.* B **37** 4441
[18] Ferconi M and Tosi M P 1991 *Europhys. Lett.* **14** 797

[19] Lebowitz J L and Percus J K 1963 *J. Math. Phys.* **4** 116
[20] Yang A J M, Fleming P D and Gibbs J H 1976 *J. Chem. Phys.* **64** 3732
[21] Coldwell-Horsfall R A and Maradudin A A 1960 *J. Math. Phys.* **1** 395
[22] Greenfield A J, Wellendorf J and Wiser N 1971 *Phys. Rev.* A **4** 1607
[23] Waseda Y 1980 *The Structure of Non-Crystalline Materials* (New York: McGraw-Hill)
[24] Landolt–Börnstein Tables 1981 vol 13 (Berlin: Springer)
[25] Woods A D B, Brockhouse B N, March R H, Stewart A T and Bowers R 1962 *Phys. Rev.* **128** 1112
[26] Cowley R A, Woods A D B and Dolling G 1966 *Phys. Rev.* **150** 487
[27] Dolling G and Meyer J 1977 *J. Phys. F: Met. Phys.* **7** 775
[28] Badirkhan Z, Rovere M and Tosi M P 1991 *J. Phys.: Condens. Matter* **3** 1627
[29] Glyde H R and Taylor R 1972 *Phys. Rev.* B **5** 1206
[30] Buyers W J L and Cowley R A 1969 *Phys. Rev.* **180** 755
[31] Fritsch G, Geipel F and Prasetyo A 1973 *J. Phys. Chem. Solids* **34** 1961
[32] Fritsch G and Bube H 1975 *Phys. Status Solidi* a **30** 571
[33] Moleko L K and Glyde H R 1984 *Phys. Rev.* B **30** 4215
[34] Zerah G and Hansen J P 1986 *J. Chem. Phys.* **84** 2336
[35] Rowlinson J S 1969 *Liquids and Liquid Mixtures* (London: Butterworths)
[36] Hansen J P and Verlet L 1969 *Phys. Rev.* **184** 151
[37] Fujii Y, Lurie N A, Pynn R and Shirane G 1974 *Phys. Rev.* B **10** 3647
[38] Batchelder D N, Haywood B C G and Saunderson D H 1971 *J. Phys. C: Solid State Phys.* **4** 910
[39] Klein M L, Barker J A and Koehler T R 1971 *Phys. Rev.* B **4** 1983
[40] Gewurtz S and Stoicheff B P 1974 *Phys. Rev.* B **10** 3487
[41] Holt A C, Hoover W G, Gray S G and Shortle D R 1970 *Physica* **49** 61
[42] Klein M L and Murphy R D 1972 *Phys. Rev.* B **6** 2433
[43] DeWitt H E, Slattery W L and Stringfellow G S 1990 *Strongly Coupled Plasma Physics* ed S Ichimaru (Tokyo: Yamada Science Foundation) p 635
[44] Helfer H L, McCrory R L and Van Horn H M 1984 *J. Stat. Phys.* **37** 577
[45] Chaturvedi D K, Senatore G and Tosi M P 1981 *Nuovo Cimento* B **62** 375
[46] Pollock E L and Hansen J P 1973 *Phys. Rev.* A **8** 3110
[47] Van Horn H M 1969 *Phys. Lett.* A **28** 706
[48] Carr W J Jr 1961 *Phys. Rev.* **122** 1437
[49] Clark C B 1958 *Phys. Rev.* **109** 1133
[50] Kugler A A 1969 *Ann. Phys.* **53** 133
[51] Ogata S and Ichimaru S 1990 *Phys. Rev.* A **42** 4867
[52] Barrat J L, Hansen J P and Pastore G 1988 *Molec. Phys.* **63** 747
[53] Curtin W A and Ashcroft N W 1985 *Phys. Rev.* A **32** 2909
[54] Curtin W A 1988 *J. Chem. Phys.* **88** 7050
[55] Denton A R and Ashcroft N W 1989 *Phys. Rev.* A **39** 426
[56] Ferconi M 1991 *ICTP Internal Report*